Low-density parity-check codes for volume holographic memory systems

Hossein Pishro-Nik, Nazanin Rahnavard, Jeongseok Ha, Faramarz Fekri, and Ali Adibi

We investigate the application of low-density parity-check (LDPC) codes in volume holographic memory (VHM) systems. We show that a carefully designed irregular LDPC code has a very good performance in VHM systems. We optimize high-rate LDPC codes for the nonuniform error pattern in holographic memories to reduce the bit error rate extensively. The prior knowledge of noise distribution is used for designing as well as decoding the LDPC codes. We show that these codes have a superior performance to that of Reed–Solomon (RS) codes and regular LDPC counterparts. Our simulation shows that we can increase the maximum storage capacity of holographic memories by more than 50 percent if we use irregular LDPC codes with soft-decision decoding instead of conventionally employed RS codes with hard-decision decoding. The performance of these LDPC codes is close to the information theoretic capacity. © 2003 Optical Society of America

OCIS codes: 210.2860, 200.3050.

1. Introduction

Holographic memories have been of intense interest recently due to their potentials for large storage capacity and fast data access. Recently, a lot of research has been done on holographic storage systems, and several demonstrations of holographic memory systems have been reported.[1–5] The information in a holographic memory system is recorded and retrieved in the form of two-dimensional data pages, i.e., two-dimensional patterns of bits. During the recording of a page, a signal beam is formed by modulating a plane wave that is generated by a spatial light modulator. The interference of this signal beam with a reference beam is recorded in a recording medium. Several pages (at least 1000) are multiplexed in a holographic memory module by use of distinct reference beams for distinct data pages. Multiplexing of up to 10,000 holograms has been reported.[6] Readout of a desired page is performed by the reference beam corresponding to that page. The diffraction of the reference beam off the hologram onto a camera (CCD or complementary metal-oxide

semiconductor) results in the retrieval of the data page. The parallelism during recording and readout due to the page-oriented nature of holographic memories results in large recording and readout rates. The possibility of multiplexing several holograms in the same volume results in considerable data storage capacities. The recent advances in SLM and CCD technologies play a major role in the success of holographic memories as both the storage capacity and the data transfer rates scale linearly with the number of bits per page. Currently both SLMs and CCDs with at least 1024×1024 pixels are available resulting in 1 Mbit pages. Multiplexing 1000 of such pages in a memory module (typical size of the recording material: 1 cm^3) results in a capacity of 1 Gbit. A modest frame rate of 1 kHz during readout results in 1 Gbit/s data rate. With advances in both recording materials (which allows multiplexing more holograms) and the SLM and CCD technologies (that allow more pixels per page and larger frame rates), improvement by at least one order of magnitude in both the storage capacity and the data transfer rate is expected in the near future.

The capacity of a holographic memory system is controlled by the number of pages and the number of information bits per page. The number of pages (or holograms) is usually determined by the dynamic range of the recording materials. Multiplexing more holograms results in weaker holograms and lower signal-to-noise ratio(s) (SNR)(s). If M holograms are multiplexed appropriately, the diffraction

efficiency (η) of each hologram is given by $\eta = [(M/\#)/M]^2$, with $M/\#$ being the dynamic range parameter.[7] Use of weak holograms (corresponding to large number of pages) results in large raw bit error rate (BER) (typically $10^{-5} - 10^{-3}$). This is much higher than the practically required BER of 10^{-12}. This makes the use of error correcting codes inevitable. The use of strong error correcting codes results in a smaller number of information bits per page due to larger number of parity bits added for error correction. However, because larger raw BERs are acceptable for stronger codes the number of pages is increased. Therefore, for a given error correcting code, there is an optimum number of holograms that results in the maximum storage capacity. This optimum depends on several parameters including the noise characteristics of the systems, the dynamic range parameter ($M/\#$), and the error correcting code. Read-Solomon (RS) codes and modulation codes have been extensively used for holographic memory systems.[8–10] The detailed optimization of the storage capacity of holographic memory systems using RS codes has been reported.[8] Soft-decision array decoding and parallel detection for page-oriented optical memories have been studied also.[11,12]

The noise characteristics and therefore, BER in holographic memories is not uniform over a data page. Typically, the probability of error is minimum at the center of the page and increases by increasing the distance from the center of the page[8] (BER is highest at the corners of the page). Typically, the raw BER might vary by two orders of magnitude over a page. Therefore, we need to design a nonuniform error protection scheme. Chou and Neifeld proposed an interleaving scheme to deal with the nonuniform error pattern arising from random and systematic errors.[8] They could increase the storage capacity by their interleaving method.

An excellent candidate for nonuniform error protection in holographic memory systems is the family of low-density parity-check (LDPC) codes. Our focus in this paper is to show the potentials of LDPC codes for holographic memory systems. We compare the performance of a typical storage system incorporating the LDPC codes with that incorporating the RS codes. We use a holographic system similar to that previously used for the optimization of the memory systems with the RS codes reported in Ref. 8. We perform the optimization for the same system with the LDPC codes. Although we concentrate on the LDPC codes for holographic memory systems, the coding method presented here is general and can be applied to other page-oriented memory systems.

In this paper we propose a method to design good LDPC codes for volume holographic memory (VHM) systems. In Section 2 we briefly discuss soft- and hard-decision decoding of error-correcting codes (ECC). In Section 3 we first explain why LDPC codes are suitable for holographic memory systems and then discuss the design of LDPC codes for these systems. In Section 4 we show the results of Monte Carlo simulation for estimating the performance of

these codes and compare these results with that of RS codes. Final conclusions are summarized in Section 5.

2. Error-Correcting Codes for Volume Holographic Memory Systems

Error correcting codes (ECC) have been applied to VHM to increase the storage capacity of the system. Storage capacity is defined as the number of information bits stored under the condition that the BER is lower than a required value. The information theoretic capacity can be considered as an upper bound for the storage capacity. Because the diffraction efficiency of the recorded holograms decreases with an increase in the number of pages, the BER increases when we increase the number of stored pages. To increase the storage capacity, we can store more pages and use ECC to decrease the BER to the desired value. If we increase the number of stored pages by a factor f, the capacity of the system is increased by the factor $f \times R$, where R is the code rate (the ratio of the number of information bits to the total number of bits). Thus, for a constant number of pages, to have the highest storage capacity we need to find a code with highest rate that provides us with the required output BER. The optimization of the number of pages was studied in Ref. 8. Here we first assume a fixed number of pages and try to design codes for VHM with R as large as possible while keeping the BER constant. Then we change the number of pages and try to maximize the storage capacity.

The decoder of an ECC can be a soft-decision decoder or a hard-decision decoder. In the hard-decision decoding, inputs to the decoder are binary-valued bits. Unlike the hard-decision decoding, the inputs in the soft-decision decoding are real numbers (in practice an analog-to-digital converter is used to quantize the input to a finite number of levels). Consider a VHM system in which we assume all pixels are independent. Note that in reality, pixels are not independent, however, we make this assumption to make our analysis easier. The information theoretic capacity of this system is equal to

$$C = M \sum_{i=1}^{N^2} C_i, \qquad (1)$$

where M is the number of stored pages, N^2 is the number of pixels in a page, and C_i is the capacity of the channel seen by the ith pixel. Note that C_i depends on M. If we have access to only hard information of the output of the channel, then the channel can be considered as N^2 parallel binary symmetric channels (BSC). The information theoretic capacity of this channel model is

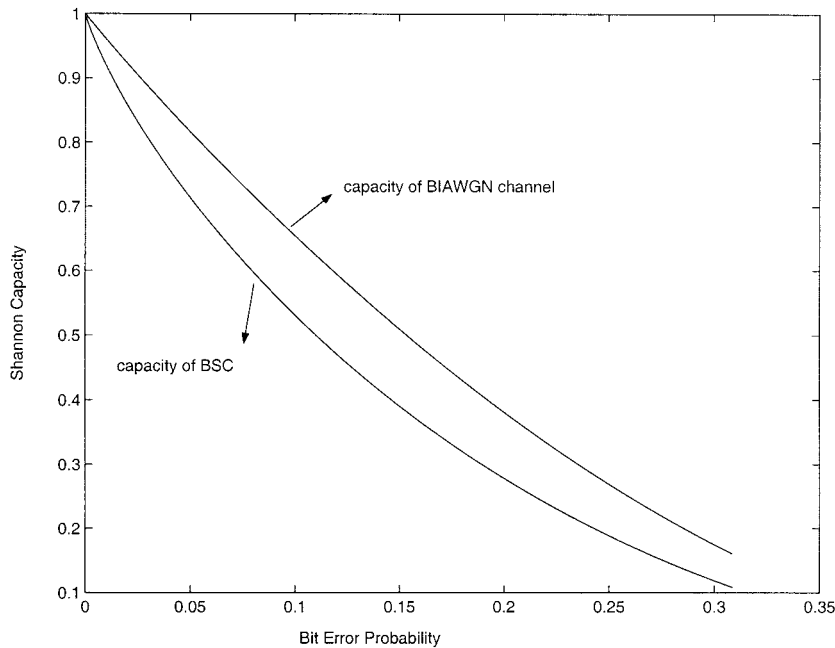$$C = M \sum_{i=1}^{N^2} C_i = M \sum_{i=1}^{N^2} [1 - H(p_i)], \qquad (2)$$

Fig. 1. Capacity of the BSC and the BIWAGN channel versus the bit error probability.

where p_i is the probability of error of the ith bit and H is the binary entropy function given by

$$H(p) = p \, \log_2\left(\frac{1}{p}\right) + (1 - p)\log_2\left(\frac{1}{1 - p}\right). \quad (3)$$

However, if we have access to the soft information in the decoder and if we assume the additive white Gaussian noise approximation, then the channel can be modeled as N^2 parallel binary input additive white Gaussian noise (BIAWGN) channels for which the capacity C_i is given by[13]

$$C_i = -\int \phi_i(x)\log_2[\phi_i(x)]dx - \frac{1}{2} \, \log_2(2\pi e\sigma_i{}^2). \quad (4)$$

Here, we have

$$\phi_i(x) = \frac{1}{\sqrt{8\pi\sigma_i{}^2}} \left(e^{-\frac{(x+1)^2}{2\sigma_i{}^2}} + e^{-\frac{(x-1)^2}{2\sigma_i{}^2}}\right), \quad (5)$$

where σ_i is the variance of the noise that affects the ith bit. Figure 1 depicts the capacity of the BIAWGN and BSC channels versus the bit error probability. Obviously, the capacity of the BIAWGN channel is higher than that of the BSC with the same bit error probability, because in the BIAWGN channel we have more information about the output of the channel. There exist both soft- and hard-decision decoding algorithms for LDPC codes.[13,14] To have the best BER performance, we choose to perform soft-decision decoding as we explain later.

3. Low-Density Parity-Check Codes for Volume Holographic Memory Systems

A. Background on Low-Density Parity-Check Codes

LDPC codes were first proposed by Galleger.[14] Recently, these codes were rediscovered and improved.[13,15–20] An LDPC code is defined as a linear block code with a sparse parity-check matrix $H = [h_{ij}]$, i.e., most of the elements of H are equal to 0 and a few of them are equal to 1. For a (k, n) binary linear block code, the parity-check matrix has $m = n - k$ rows and n columns, and codewords x are binary vectors of length n that satisfy the equation $Hx = 0$. Each row of H corresponds to a parity-check equation and each column corresponds to one bit of the codewords. An LDPC code can also be represented by a bipartite graph called the Tanner graph.[21] A Tanner graph is a bipartite graph with bipartition V and C, where $V = \{v_1, v_2, \ldots, v_n\}$ is the set of variable (message) nodes and $C = \{c_1, c_2, \ldots, c_m\}$ is the set of check nodes. The nodes c_i and v_j are adjacent (connected by an edge) if and only if $h_{ij} = 1$. The degree of a node is defined as the number of edges incident with it. An LDPC code is called regular if the degrees of all message nodes are equal and the degrees of all check nodes are equal. Otherwise the code is called irregular. As an example, Fig. 2 shows the Tanner graph of the code defined by

$$H = \begin{pmatrix} 1 & 1 & 0 & 1 & 0 & 0 \\ 0 & 1 & 1 & 0 & 1 & 0 \\ 1 & 0 & 1 & 0 & 0 & 1 \end{pmatrix}. \quad (6)$$

It is clear from Fig. 2 that the code is irregular because the variable nodes have different degrees. As we see later, this irregularity will be exploited to construct nonuniform ECC.
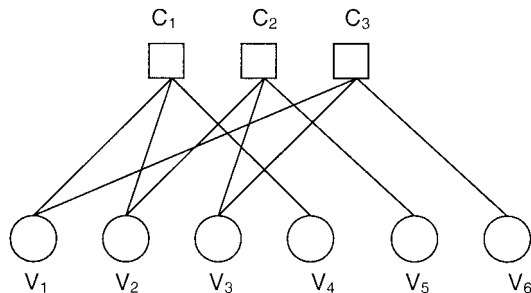
Fig. 2. Tanner graph for an LDPC code.

LDPC codes can be decoded by iterative algorithms called message-passing algorithms. In these algorithms, messages are exchanged between variable nodes and check nodes iteratively. In each iteration, every check node c receives messages from all its neighbor variable nodes (two vertices are neighbors if they are adjacent). Based on these messages, the check node computes new messages and sends them to its neighbors. A message that the check node c sends to a variable node v is a function of the incoming messages from all neighbors of c except v. Similarly, variable nodes send messages to their neighbor check nodes. In this paper we consider a message passing algorithm that is called the belief propagation. Therefore, to perform the decoding, we need to know the update equations for the belief propagation algorithm. The detail of this algorithm can be found in Ref. 13.

Richardson *et al*. developed an algorithm, called density evolution to find the densities of the messages exchanged between variable nodes and check nodes.[13,16] In this method, the distributions of messages from variable nodes to check nodes at two consecutive iterations of belief propagation are connected by a recursive formula. They used this method to determine the performance of LDPC codes and to find optimum degree distributions for LDPC codes. Here we will use similar formulas for the nonuniform error patterns in VHMs.[22]

B. Low-Density Parity-Check Codes for Volume Holographic Memory

LDPC codes are suitable for holographic memories for a variety of reasons. First, it is shown that they have a performance near Shannon limit.[13,16,18] Therefore, we will be able to approach the information theoretic capacity of the channel using LDPC codes, while RS codes do not have a performance near the information theoretic capacity for the practically limited block length. Second, not only do we use the prior knowledge of the noise distribution in the VHM data page in designing the code, but also we use this information in the decoding period. On the contrary, it is not easy (if not impossible) to incorporate the prior knowledge of noise distribution into the designing and decoding of RS codes. An interesting method was proposed in Ref. 8 to cope with the nonuniform noise distribution. The authors suggested interleaving the bits such that all message blocks contain the same number of good bits and bad bits (bits with low noise and bits with high noise). In other words, the average noise power in a message block after interleaving is independent of the location of bits. However, we still cannot use the prior information about noise distribution at the decoding step.

In the design of LDPC codes we use the flexibility of these codes for choosing the degree distribution of the Tanner graph. We choose the degree distribution such that the code performance is optimized for the channel noise distribution. In the decoding process, we use log-likelihood ratios that contain the information about the noise power for a specific bit and the information about how reliably that bit was transmitted across the channel. Third, the decoding of LDPC codes is fully parallelizable and very fast, which makes these codes desirable for VHM systems. This enables us to use a long block length and decrease the BER while we maintain lower redundancy.

The main drawback of LDPC codes is that they have a slow encoder. This is not a problem in the VHM systems because we use a high-rate LDPC code with a systematic encoder. Therefore, we need to encode only parity bits whose number is a small fraction of the block length. Moreover, we can also use the method described in Ref. 17 to simplify the encoding process.

Another problem with LDPC codes is that they may show an error floor effect. However, not all LDPC codes have this property. For example, for the LDPC codes that we designed in this paper, we did not observe any error floor down to the BER of 10^{-9}. Additionally, these codes perform close to the Shannon capacity. An alternative technique to deal with an error floor is to concatenate an outer code with an LDPC code. This way, we can decrease error probability significantly, with a small loss of the storage capacity. However, an interleaver is required to distribute the errors in an erroneous LDPC word to several words of the outer code.

We mention that when we change the number of pages, we need to design a new LDPC code with a different degree distribution so that the code is optimized for the new channel. However, this is not a problem because the code is designed off-line. Moreover, this flexibility of LDPC codes enables us to optimize the code for each specific channel. On the contrary, for the RS codes over $GF(q)[GF(q)$ is the finite field with q elements], there is no need for designing because there is no design parameter, except the rate.

C. Design of Nonuniform Error Correcting Low-Density Parity-Check Codes

In this section we briefly discuss the design of efficient LDPC codes for holographic memories. An irregular LDPC code ensemble is specified by its degree distribution.[16,20] The degree sequence determines the percentage of variable or check nodes of different degrees. It is shown in Ref. 13 that the performance of a randomly chosen LDPC code from an ensemble of

LDPC codes with a given degree sequence is very close to the average performance of the codes in the ensemble with a high probability. The nonuniform error pattern of holographic memories suggests using irregular LDPC codes. One approach is to find the average noise distribution over the page and to design a good degree sequence for the resulting channel. However, we consider another approach that is more suitable for nonuniform error correction. The details of this design method are described in Ref. 22. Here, we only describe the main idea. As was shown in Ref. 8, each page can be divided into k_r regions whose bits have a similar BER. Generally, pixels at the corner of a data page have a higher probability of error than those at the center of the page. Suppose the constant BER regions are $R_1, R_2, \ldots, R_{k_r}$. Let n be the block length and $(x_1, x_2, \ldots, x_n)$ be a codeword. Also, let $W^{(j)}$ be the set of the bits in the jth region in the codeword, i.e., $W^{(j)} = \{x_i : x_i \in R_j\}$, and $|W^{(j)}| = n^{(j)}$, where $|\cdot|$ denotes the cardinality of a set. Roughly speaking, instead of assuming a single degree distribution for all nodes, we consider the ensemble of graphs in which the bits from different regions may have different degree distributions.

To optimize LDPC codes for the nonuniform error protection, we then find the density evolution formulas for these codes.[22] For simplicity, we can use a Gaussian approximation method[19] (if we assume Gaussian noise). As in the uniform error protection case, we need to have only a few nonzero coefficients for the degree distributions of the variable nodes and check nodes[16,20,22] to find the good degree distributions. In fact, we observed that we can find good degree distributions by the following simple scheme: We let all the variable nodes of the same type [all bits that lie in $W^{(j)}$] have the same degree, and the degree distribution of the check nodes is concentrated at one degree or at two consecutive degrees.

We now undertake some important issues about the design of these codes. Let us consider the encoding problem. Because an LDPC code is used with very large lengths, its generator matrix has large dimensions. This requires a large number of computations in the encoding algorithm. To avoid this, we use the generator matrix G in the systematic form. This means that if we encode a vector $(u_1, u_2, \ldots, u_k)$ to a codeword $(x_1, x_2, \ldots, x_n)$ we have $u_i = x_i$ for $1 \le i \le k$. Therefore, we need to calculate only $n - k$ bits $x_{k+1}, x_{k+2}, \ldots, x_n$. Because in holographic memories, we usually use high-rate codes, $n - k$ is a small number that results in less computation with respect to nonsystematic encoding.

Another issue is avoiding short cycles in the Tanner graph of the code. To have a good performance, we need to avoid short cycles (cycles of four in length) in the Tanner graph.[14,15] Unfortunately, the higher the code rate is, the more difficult (if not impossible) it is to eliminate these cycles. Because we use high-rate codes in holographic memories, it is likely that there exists several short cycles in the Tanner graph representation of the code. We avoided these short cycles as much as possible. We also maintained the
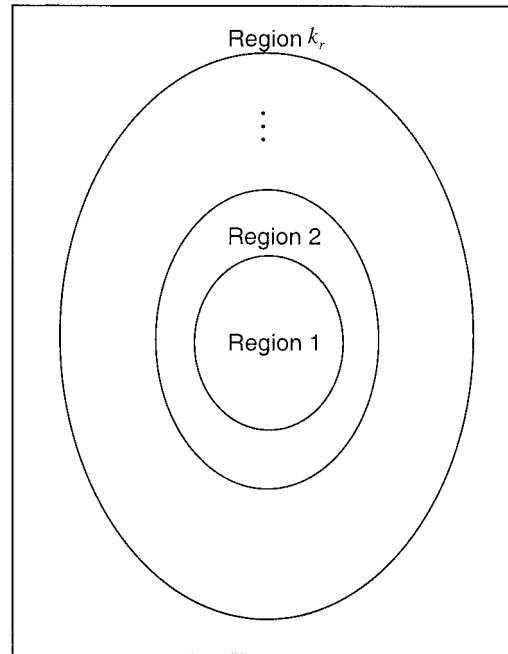

Fig. 3. Different regions in a typical data page in holographic recording. Raw BER is almost constant in each region.

graph to be very sparse (less than one percent of the elements of the parity-check matrix are one) (by choosing a very sparse parity check matrix) to avoid the short cycles.

We would like to point out that in Ref. 11, those authors proposed a likelihood-based two-dimensional equalization for extenuating interpixel interference noise in VHM systems and combined it with the soft-decision of the array codes. A similar scheme can be used for LDPC codes as well to improve the performance of the code further. The decoding algorithm for LDPC codes in intersymbol interference channels is described in Ref. 23.

4. Simulation Results

We implemented the LDPC codes that we designed to examine their performance. For simulation we chose a system similar to Ref. 8. As explained in Ref. 8, different kinds of errors are present in the system. The probability density function of the noise is determined by considering the effect of all these error sources. For simplicity, we assume that the noise is additive white Gaussian and its variance is a function of the pixel location. Note that the formulas used in decoding and density evolution are quite general and can be applied to any symmetric[13] noise distribution. Therefore, our analysis can be applied to any system with a nonuniform error pattern. As mentioned before, the raw BER in volume holographic storage depends on the position of the bit in the data page. Figure 3 shows the different regions with a constant raw BER before error correction. In each region, pixels have almost the same probability of error.[8] In our simulations we divided a page into four regions. We assume the system has
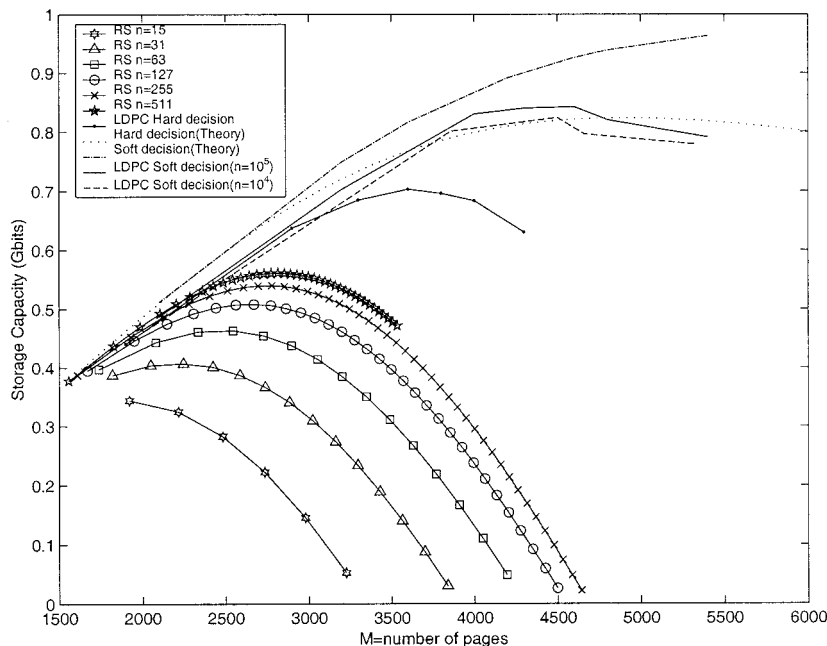
Fig. 4. Comparison of different coding schemes for VHMs.

a raw BER approximately from 10^{-3} to 10^{-6} when 2000 pages are stored. This raw BER increases when the number of pages increases. Similar to Ref. 8, we make the following assumption: The magnitudes of the systematic error and the thermal noise are assumed to remain unchanged with respect to M (the number of pages) and SNR per pixel can be computed by using the scaling law that states that the SNR is proportional to $(1/M^2)$.[8,24]

Normally, the output BER of 10^{-12} is desirable for the holographic storage. However, because of the extensive computation that is involved to find the performance of the code at 10^{-12}, we are compelled to obtain an upper bound on the BER. Because it is computationally feasible to decode 10^9 bits, we performed our experiments for this number of bits. For an optimized LDPC code of a given rate we found the maximum number of pages such that after the decoding of 10^9 bits, no error was observed. We then concluded that the average BER was upper bounded by 10^{-8}. We also considered RS codes of several different lengths ranging from 15 to 511 and determined the number of pages for the output BER of 10^{-8}. We anticipate that if the actual error rate for the LDPC code is higher than 10^{-12}, we can reach the BER of 10^{-12} by very subtle reduction in the capacity provided we do not face an error floor problem. The reason for this is that LDPC codes are known to have a threshold effect.[13] For a given degree of distribution, this threshold can be defined as the maximum possible noise level, to have reliable communication. Equivalently, we can define the SNR threshold as the minimum SNR required for reliable communication. If the SNR is higher than the SNR threshold, we can achieve an arbitrary small probability of error if we are allowed to have a high enough block length.

However, if the SNR is lower than the SNR threshold, the probability of error is bounded away from zero by a strictly positive constant. As long as we use these codes for a channel with an SNR higher than the threshold, increasing the SNR by a small value results in a drastic reduction of the BER.[18] Because we use these codes just below their noise threshold (or above the SNR threshold), we expect that even if our codes have a BER higher than 10^{-12}, we can reach this error rate by reducing the number of pages slightly. The above discussion is valid if the code does not have an error floor higher than 10^{-12}. In a case when we cannot avoid the error floor, as we mentioned, we can concatenate an outer code with the LDPC code.

Figure 4 shows the storage capacity that is obtained by using LDPC codes and RS codes of different lengths and different decoding methods. For RS codes, we used the same interleaving scheme that was proposed in Ref. 8 to improve the performance of the code for the nonuniform noise distribution. Only hard-decision decoding is considered for RS codes. The maximum storage capacity that is gained by using RS codes is 0.5609 Gbits, which is obtained when an RS code of length 511 is used and 2802 pages are stored. The maximum storage capacity that is obtained by using LDPC codes is 0.8423 Gbits. This is achieved when 4600 pages are stored and the soft LDPC decoder is used. We note that this capacity is about 50 percent higher than that of the RS codes. This sizable increase in the capacity by the LDPC code can be explained by use of Fig. 4. When the number of pages is small, there is not much difference between the RS codes and the LDPC codes. This is because the information theoretic capacity of hard-decision and soft-decision decoding are close to each
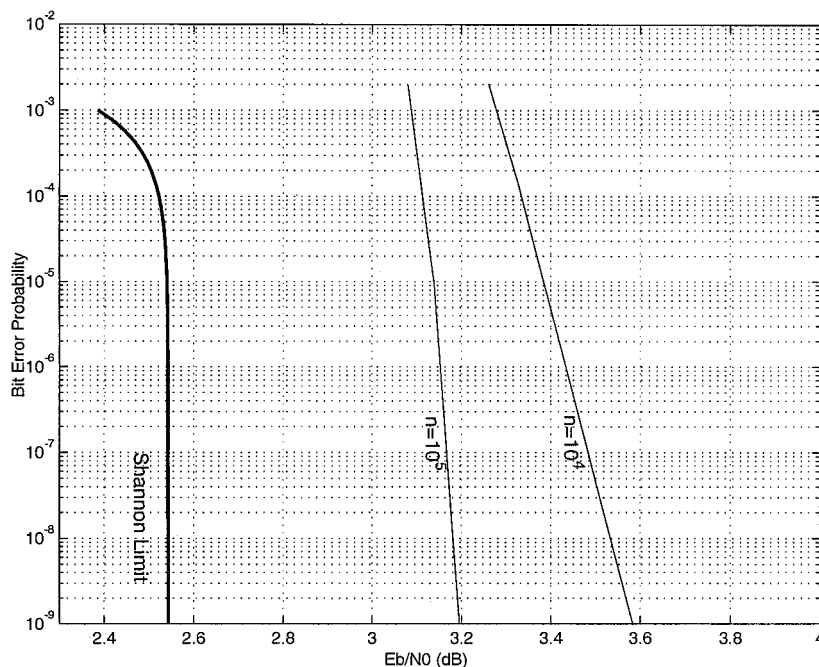
Fig. 5. Performance of the irregular LDPC code of rate 0.85.

other for a high SNR [or equivalently, a small number of pages (Fig. 1)]. Moreover, RS codes have a good performance for such SNRs. However, when the number of pages increases and therefore SNR decreases, the difference between the capacity of hard-decision and soft-decision decoding increases. More importantly, LDPC codes maintain near the Shannon limit of performance for the low SNR, while the performance of RS codes is far from the Shannon limit in the low SNR. For this reason, the optimum number of pages for LDPC codes is higher than that for RS codes. We also note that the performance of LDPC codes with hard-decision decoding is about 25 percent higher than the maximum capacity of the RS codes.

It is important to note that the full advantage of LDPC codes is obtained if we choose the optimum number of holograms ($M \simeq 4600$). The number of holograms that can be recorded in a recording material (for example, a photorefractive crystal) is limited by the finite dynamic range and the angular selectivity. By use of a 1-cm thick $LiNbO_3$ crystal with the current values of $M/\#$, it is possible to multiplex several thousand holograms. Two reported examples are 5000 and 10,000 holograms.[6,25] If for any reason (thin crystal, small $M/\#$, large noise level, etc.) the maximum number of holograms is below 2000, the advantage of LDPC codes will be lost as evidenced by Fig. 4.

Let us now specifically give one of the codes that we found. For the rate 0.85 we divided the page into four different regions (region one to four) each with a different noise power. Consider the code for which we have

$$d_1 = 3, \ d_2 = 4, \ d_3 = 7, \ d_4 = 10, \ d_c = 40, \quad (7)$$

where d_i is the degree of variable nodes of the bits from region i, and d_c is the degree of check nodes. Note that the degree distribution is very simple. The relative SNRs in different regions are

$$SNR_2 - SNR_1 = 1.61dB,$$
$$SNR_3 - SNR_1 = 2.80dB,$$
$$SNR_4 - SNR_1 = 3.74dB. \quad (8)$$

Figure 5 shows the performance of this code when the block length is $n = 10,000$ and $n = 100,000$. It can be noticed from the figure that for $n = 100,000$ at the BER of 10^{-9} the gap from the capacity is only 0.65 dB and for $n = 10,000$ this gap is 1.04 dB. Moreover, the codes do not present any error floor at least for the BERs higher than 10^{-9}. We think that having a degree distribution that is close to regular (bits from the same regions have the same degree) helps to mitigate the error floor problem. Obviously, it is possible to find a more complicated degree sequence and get closer to the Shannon capacity. But, in this case, we may have an error floor problem. We see that the simple scheme that we propose here is close enough to the information theoretic capacity and yet does not have the error floor problem.

Figure 6 presents the performance of the optimized irregular LDPC codes in comparison with the maximum possible rate determined by information theory to have reliable communication on the channel (Shannon's capacity). We see that the LDPC code rates are close to the capacity limit. We have chosen the code rate below the theoretic threshold to ensure that the probability of the error is less than 10^{-8}.

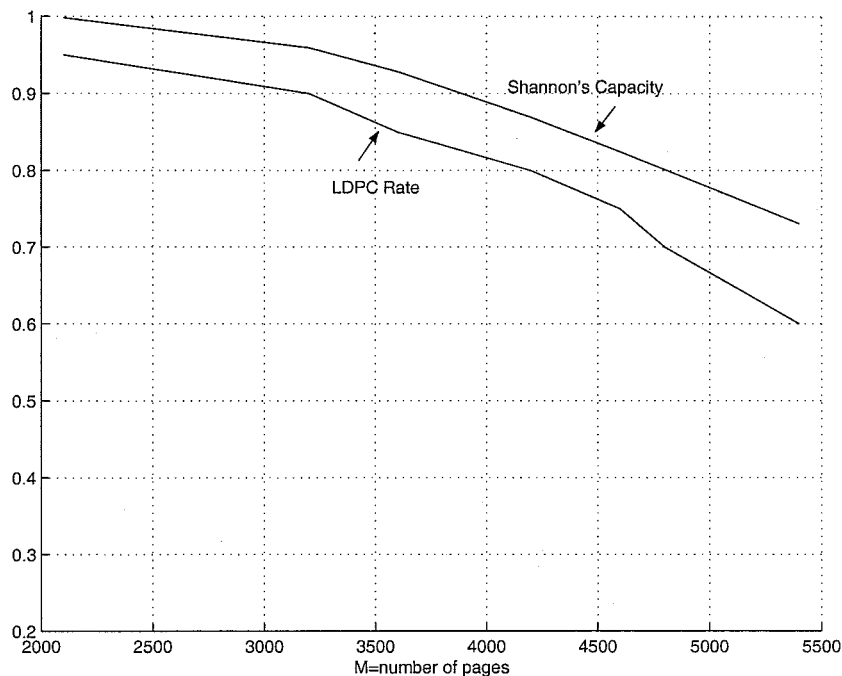In Fig. 7 we compare our irregular LDPC code with

Fig. 6. Comparison of the performance of irregular LDPC code with Shannon's capacity of the channel.

a regular one. We chose an irregular LDPC code of rate 0.85 that is optimized for our system and compared its performance with a regular LDPC code of the same rate. We changed the number of pages and computed the output BER for both codes. For each number of pages we decoded a stream of 10^7 bits and computed the average BER. The average BER is plotted in Fig. 7. The threshold effect of LDPC codes can be seen from Fig. 7. Here, we can define the threshold of an LDPC code as the maximum number of pages for which the BER can be made very

small. By this definition, the threshold of the regular code is $M \simeq 3000$, while the threshold of the irregular one is $M \simeq 4000$. This indicates that we can increase the storage capacity by 34 percent by using the irregular LDPC code instead of a regular one. Note that the code rate for the two codes in Fig. 7 are the same.

Figure 8 presents the error probability of the designed LDPC code for different iterations in decoding. We chose an irregular LDPC code of rate $R = 0.9$ with $M = 3400$. We computed the average BER
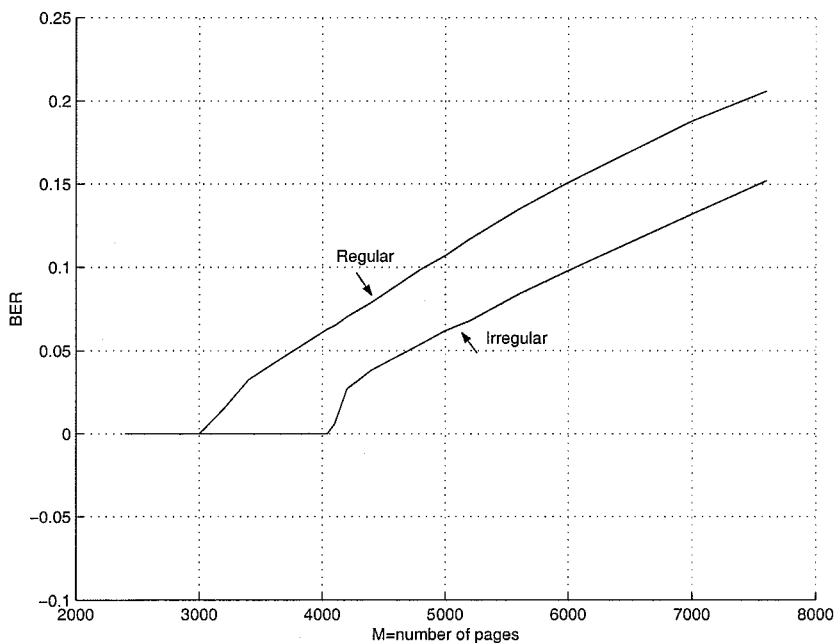

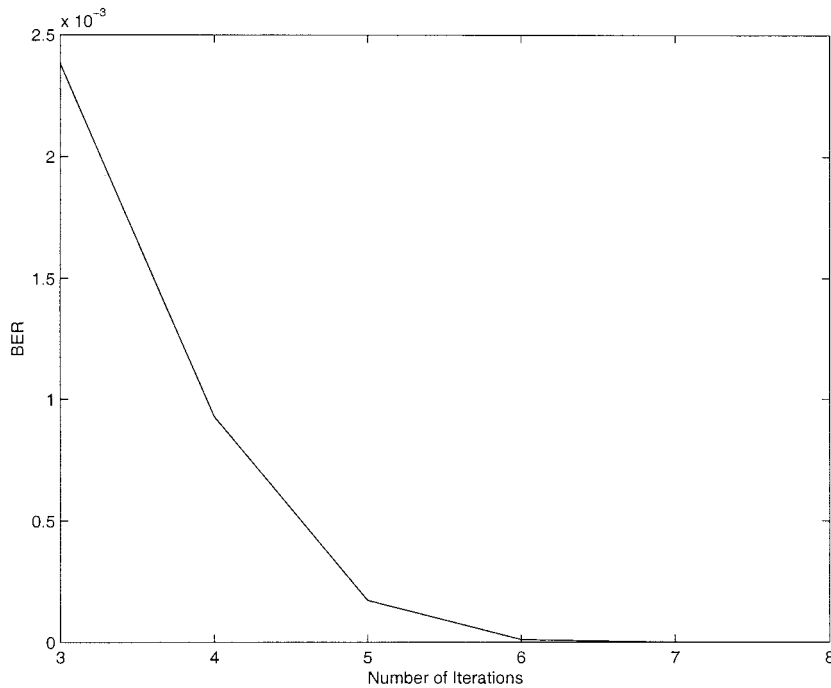Fig. 7. Comparison of the performance of irregular and regular LDPC codes.

Fig. 8. Performance of the irregular LDPC code for different iterations.

for different iterations by decoding 10^7 bits. We observed no error after the 8th iteration. This shows that usually a few iterations are sufficient to correct all errors and therefore, the decoding is very fast. This is because we use LDPC codes below their noise threshold and moreover, usually the SNR in VHMs is high, so a small fraction of received bits are in error.

Figure 9 presents the BER as a function of the number of pages for different values of n (block length) for LDPC codes of rate 0.95. We observe that the BER decreases as n increases. This is expected, because codes with higher block lengths demonstrate better performance. However, as we increase n, the complexity of encoding and decoding increases accordingly. Therefore, we should utilize
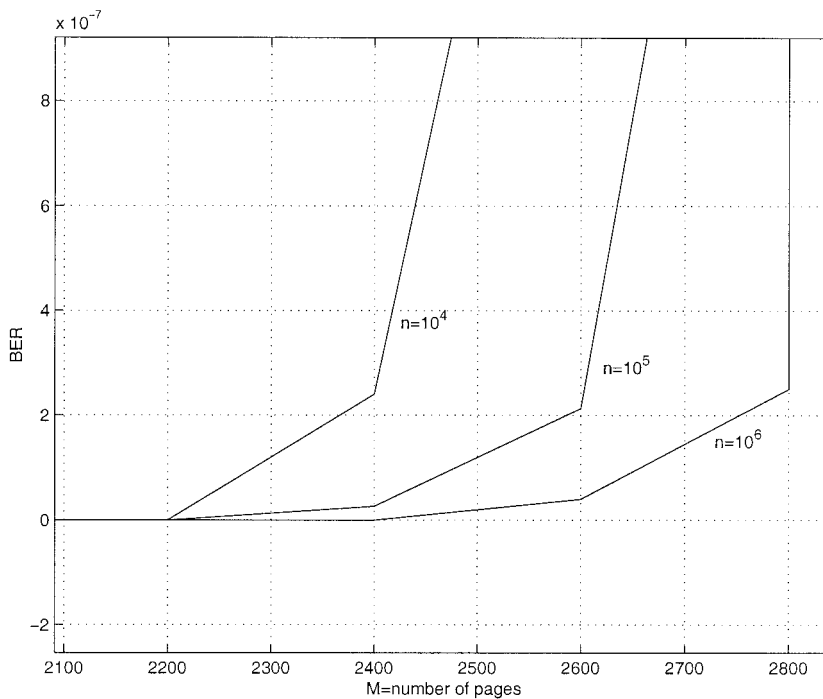

Fig. 9. Performance of irregular LDPC codes with different block lengths.

an optimum value of n with acceptable performance and complexity.

5. Conclusion

We studied the application of LDPC codes for VHM systems. We proposed a method to design irregular LDPC codes for holographic memories in which the noise is nonuniformly distributed. Our method is based on the fact that different pixels of a page are subject to the different noise probability density functions. We used a generalized density evolution technique to design optimal irregular LDPC codes. We compared the performance of the irregular LDPC codes with that of the RS codes of different lengths. We showed that we can increase the storage capacity considerably by using an irregular LDPC code that is optimized for the nonuniform noise distribution. We also showed that the optimized irregular codes have better performance than regular codes. Although this is true in general, the fact that the channel noise has a nonuniform distribution strengthens this phenomenon.

References

1. J. F. Heanue, M. C. Bashaw, and L. Hesselink, "Volume holographic storage and retrieval of digital data," Science **265,** 749–752 (1994).
2. D. Psaltis and F. Mok, "Holographic memories," Sci. Am. **273,** 70–76 (1995).
3. I. McMichael, W. Christian, D. Pletcher, T. Y. Chang, and J. H. Hong, "Compact holographic storage demonstrator with rapid access," Appl. Opt. **35,** 2375–2379 (1996).
4. R. M. Shelby, J. A. Hoffnagle, G. W. Burr, C. M. Jefferson, M.-P. Bernal, H. Coufal, R. K. Grygier, H. G. Unther, R. M. Macfarlane, and G. T. Sincerbox, "Pixel-matched holographic data storage with megabit pages," Opt. Lett. **22,** 1509–1511 (1997).
5. G. W. Burr, C. M. Jefferson, H. Coufal, M. Jurich, J. A. Hoffnagle, R. M. Macfarlane, and R. M. Shelby, "Volume holographic data storage at areal density of 250 gigapixels/in.^{2}," Opt. Lett. **26,** 444–446 (2001).
6. X. An, G. W. Burr, and D. Psaltis, "Thermal fixing of 10,000 holograms in linbo$_3$:Fe," Appl. Opt. **38,** 386–393 (1999).
7. G. B. F. Mok and D. Psaltis, "System metric for holographic memory systems," Opt. Lett. **21,** 896–898 (1996).
8. W. Chou and M. A. Neifeld, "Interleaving and error correction in volume holographic memory systems," Appl. Opt. **37,** 6951–6968 (1998).
9. G. W. Burr, J. Ashley, H. Coufal, R. K. Grygier, J. A. Hoffnagle, C. M. Jefferson, and B. Marcus, "Modulation coding for pixel-matched holographic data storage," Opt. Lett. **22,** 639–641 (1997).
10. M. A. Neifeld and W. Chou, "Information theoretic limits to the capacity of volume holographic optical memory," Appl. Opt. **36,** 514–517 (1997).
11. W. Chou and M. A. Neifeld, "Soft-decision array decoding for volume holographic memory systems," J. Opt. Soc. Am. A **18,** 185–194 (2001).
12. X. Chen, K. M. Chugg, and M. A. Neifeld, "Near optimal parallel distributed data detection for page-oriented optical memories," IEEE J. Sel. Top. Quantum Electron. **4,** 866–879 (1998).
13. T. J. Richardson and R. L. Urbanke, "The capacity of low-density parity-check codes under message-passing decoding," IEEE Trans. Inf. Theory **47,** 599–618 (2001).
14. R. G. Galleger, *Low-density Parity-Check Codes* (MIT, Cambridge, Mass., 1963).
15. D. J. C. MacKay, "Good error-correcting codes based on very sparse matrices," IEEE Trans. Inf. Theory **45,** 399–431 (1999).
16. T. J. Richardson, M. A. Shokrollahi, and R. L. Urbanke, "Design of capacity-approaching irregular low-density parity-check codes," IEEE Trans. Inf. Theory **47,** 619–637 (2001).
17. T. J. Richardson and R. L. Urbanke, "Efficient encoding of low-density parity-check codes," IEEE Trans. Inf. Theory **47,** 638–656 (2001).
18. S. Y. Chung, "On the construction of some capacity-approaching coding schemes," Ph.D. dissertation (Massachusetts Institute of Technology, Cambridge, Mass., 2000).
19. S. Y. Chung, T. J. Richardson, and R. L. Urbanke, "Analysis of sum-product decoding of low-density parity-check codes using a Gaussian approximation," IEEE Trans. Inf. Theory **47,** 657–670 (2001).
20. M. Luby, M. Mitzenmacher, M. Shokrollahi, and D. Spielman, "Improved low-density parity-check codes using irregular graphs," IEEE Trans. Inf. Theory **47,** 585–598 (2001).
21. R. M. Tanner, "A recursive approach to low complexity codes," IEEE Trans. Inf. Theory **27,** 533–547 (1981).
22. H. Pishro-Nik, N. Rahnavard, and F. Fekri, "Nonuniform error correction using low-density parity-check codes," in *Proceedings of Fortieth Annual Allerton Conference on Communication, Control, and Computing*, Monticello, Ill., Oct. (2002). http://www.csl.uiuc.edu/allerton/.
23. A. Kavčić, X. Ma, and M. Mitzenmacher, "Binary inersymbol interference channels: Gallager codes, density evolution, and code performance bounds," IEEE Trans. Inf. Theory. http://www.eecs.harvard.edu/~michaelm/NEWWORK/papers.html#CodesAn.
24. D. J. Brady and D. Psaltis, "Control of volume holograms," J. Opt. Soc. Am. A **9,** 1167–1182 (1992).
25. F. Mok, "Angle-multiplexed storage of 5000 holograms in lithium-niobate," Opt. Lett. **18,** 915–917 (1993).